Solid-State ^{19}F-NMR Analysis of ^{19}F-Labeled Tryptophan in Gramicidin A in Oriented Membranes

Stephan L. Grage,* Junfeng Wang,[†] Timothy A. Cross,[†] and Anne S. Ulrich*

*Institute of Molecular Biology, 07745 Jena, Germany; and [†]National High Magnetic Field Laboratory, Tallahassee, Florida 32310 USA

ABSTRACT   The response of membrane-associated peptides toward the lipid environment or other binding partners can be monitored by solid-state NMR of suitably labeled side chains. Tryptophan is a prominent amino acid in transmembrane helices, and its ^{19}F-labeled analogues are generally biocompatible and cause little structural perturbation. Hence, we use 5F-Trp as a highly sensitive NMR probe to monitor the conformation and dynamics of the indole ring. To establish this ^{19}F-NMR strategy, gramicidin A was labeled with 5F-Trp in position 13 or 15, whose χ_1/χ_2 torsion angles are known from previous ^{2}H-NMR studies. First, the alignment of the ^{19}F chemical shift anisotropy tensor within the membrane was deduced by lineshape analysis of oriented samples. Next, the three principal axes of the ^{19}F chemical shift anisotropy tensor were assigned within the molecular frame of the indole ring. Finally, determination of χ_1/χ_2 for 5F-Trp in the lipid gel phase showed that the side chain alignment differs by up to 20° from its known conformation in the liquid crystalline state. The sensitivity gain of ^{19}F-NMR and the reduction in the amount of material was at least 10-fold compared with previous ^{2}H-NMR studies on the same system and 100-fold compared with ^{15}N-NMR.

INTRODUCTION

Because the three-dimensional structure of most membrane-bound proteins is not yet accessible, it is often useful to focus on specific molecular segments. For example, the conformation of a prosthetic group or ligand may bear functionally relevant information on a membrane-associated receptor, and the behavior of a protein side chain may yield valuable insight about its immersion in the membrane or its interaction with other binding partners. In many cases a substantial response in the conformation or motional freedom of certain side chains is expected, for example when an amphiphilic peptide associates peripherally with the lipid bilayer, when lateral protein aggregates are formed in the membrane, or when the lipid phase state is altered. These effects are readily monitored, for example, by analyzing the intrinsic fluorescence of aromatic side chains. Tryptophan (Trp) in particular is a sensitive reporter of local dynamics, hydrophobicity, and anisotropic interactions of membrane-associated proteins. For example, Raman studies and fluorescence spectroscopy have been used to monitor the alignment and environmental response of Trp side chains in gramicidin A (Scarlata, 1988, 1991; Takeuchi et al., 1990; Maruyama and Takeuchi, 1998). In other membrane proteins, Trp fluorescence spectra have been correlated with different microenvironments (Reshetnyak and Burnstein, 2001; Reshetnyak et al., 2001), and multiexponential decays have been interpreted in terms of discrete rotamer popula-

tions (Clayton and Sawyer, 1999a,b). However, the information content of such fluorescence analysis is still under debate (Ladokhin and White, 2001), as it is not straightforward to describe the absolute alignment of the Trp side chain nor to characterize its axes of motional averaging.

The only direct approach to observe the structure of a side chain in a noncrystalline membrane protein or fiber is afforded by solid-state NMR spectroscopy (Watts et al., 1995; Opella 1997; Marassi and Opella, 1998; Fu and Cross, 1999). The detailed alignment and motional averaging of specific side chains have been addressed, for example, in gramicidin A (Killian, 1992; Hu et al., 1993, 1995; Koeppe et al., 1994, 1995; Hu and Cross, 1995; Ketchem et al., 1997), bacteriorhodopsin (Spohn et al., 1983; Keniry et al., 1984), various other peripheral and transmembrane protein segments (Koenig et al., 1999; Sharpe and Grant, 2000; Sharpe et al., 2000), and silk fibers (Nicholson et al., 1993; Asakura et al., 1997; Demura et al., 1998; Kameda et al., 1999a,b). To observe a specific protein side chain by solid-state NMR, most previous studies have relied on selective isotope labeling with ^{2}H, ^{13}C, or ^{15}N, which are nonperturbing but which have an inherently low sensitivity compared with ^{1}H-NMR. To improve sensitivity, ^{19}F has been successfully used as an alternative probe in proteins, both in liquid state NMR (Gerig, 1994, 1998; Danielson and Falke, 1996; Luck et al., 1996; Sun et al., 1996; Lau and Gerig, 1997; Bouchard et al., 1998; Zemsky et al., 1999; Luck and Johnson, 2000) and solid-state NMR (McDowell et al., 1993, 1996; Feeney et al., 1996; Klug et al., 1997; Goetz et al., 1999; Ulrich 2000; Grage et al., 2001; Murphy et al., 2001; Salgado et al., 2002). In addition to its high sensitivity, which promises to reduce acquisition times theoretically by two to three orders of magnitude, ^{19}F possesses a wide dispersion of isotropic chemical shifts as well as a large chemical shift anisotropy (CSA), which renders it a highly informative reporter of local structure (Ulrich, 2000).

Having recently demonstrated the use of ^{19}F-NMR to determine the overall alignment and motional averaging of a cyclic peptide in a membrane (Grage et al., 2001; Salgado et al., 2002), here we will illustrate the structure analysis of a ^{19}F-labeled protein side chain. The most relevant candidate for this kind of investigation is ^{19}F-labeled tryptophan, besides other aromatic and aliphatic amino acids. Even though the risk of inducing a small structural or electronic perturbation cannot be completely avoided, hydrophobic side chains with a single ^{19}F-substituent at the periphery are usually compatible with the native protein structure. Fluorine-labeled Trp, Phe, and Leu are indeed the most prominent and least perturbing amino acids used for ^{19}F-NMR on proteins, as they can be readily incorporated biosynthetically by supplementing the growth medium of most expression systems (McDowell et al., 1993, 1996; Gerig 1994; Danielson and Falke, 1996; Feeney et al., 1996; Luck et al., 1996; Sun et al., 1996; Klug et al., 1997; Lau and Gerig, 1997; Bouchard et al., 1998; Goetz et al., 1999). Many studies have shown that 5F-Trp, 6F-Trp, 4F-Phe, and ωF-Leu hardly affect the surrounding protein structure (Feeney et al., 1996; Sun et al., 1996), and vice versa that the conformation of these labeled side chains hardly differs from that of the unlabeled system (Lau and Gerig, 1997; Cotten, 1998; Cotten et al., 1999).

There are several biophysical reasons why a more detailed characterization especially of Trp in membrane-associated peptides and proteins is generally desirable. Due to its amphiphilic character, Trp plays a distinguished role both in integral membrane proteins as well as in peripheral ones. In transmembrane helices Trp frequently occurs near the polar-apolar interface, where it helps to anchor the helix at an appropriate depth within the lipid bilayer (Schiffer et al., 1992; de Planque et al., 1998; Wallace and Janes, 1999; Morein et al., 2000; Rinia et al., 2000). In ion channels the dipole moments of indole rings are often aligned toward the channel center to guide the entry of ions (Hu et al., 1993, 1995; Avdonin and Hoshi, 2001; Townsley et al., 2001), and Trp may also stabilize the channel structure (Cotten et al., 1997; Okada et al., 2001). Another role of Trp has been attributed to its partial membrane immersion, which mediates the peripheral adhesion of amphiphilic peptides to membranes, as in the case of cecropins (Oh et al., 2000), indolicins (Hancock and Diamond, 2000; Friedrich et al., 2001), and annexins (Hofmann et al., 2000). In the latter example, Trp has also been suggested to modulate the formation of two-dimensional protein arrays on the membrane surface (Pigault et al., 1999). Trp side chains have been further proposed to interact with certain lipids (Killian, 1992; Mousson et al., 2001) or to facilitate the lateral association of transmembrane proteins. Hence, it is of fundamental interest to be able to monitor directly the conformation and motional behavior of this special amino acid in membrane proteins by solid-state NMR, even if this involves the observation of a nonnatural ^{19}F-substituent on the indole ring.

The alignment of a ^{19}F-labeled Trp side chain with respect to the lipid bilayer surface will be determined here by analyzing the ^{19}F CSA tensor in a uniaxially oriented membrane sample, in a similar way as it has been previously done by ^{2}H-, ^{13}C-, and ^{15}N-NMR (Spohn et al., 1983; Keniry et al., 1984; Killian 1992; Hu et al., 1993, 1995; Nicholson et al., 1993; Koeppe et al., 1994, 1995; Hu and Cross, 1995; Lee et al., 1995; Asakura et al., 1997; Demura et al., 1998; Jude et al., 1999; Kameda et al., 1999a,b; Koenig et al., 1999; Koeppe et al., 2000; Sharpe and Grant, 2000; Sharpe et al., 2000). We note that ^{19}F possesses a highly asymmetric CSA tensor, in contrast to the axially symmetric [1]H-^{15}N dipolar coupling or the nearly axially symmetric amide ^{15}N CSA and ^{2}H quadrupolar tensors. Therefore, the ^{19}F CSA tensor can be used to fully describe the three-dimensional alignment of the labeled segment with respect to the membrane normal in terms of two Euler angles, rather than providing only a single angular restraint. To extract both Euler angles, the NMR analysis requires a concerted lineshape analysis of the sample at several different tilt angles (Ulrich et al., 1992, 1994, 1995; Ulrich and Watts, 1993, 1994; Ulrich and Grage, 1998), or alternatively magic angle oriented sample spinning can be used (Glaubitz and Watts, 1998; Glaubitz et al., 1999, 2000). In principle, all tools for the analysis of ^{19}F-labels in membranes are at hand, but there remains an open question concerning 1) the principal axis values in situ and 2) the alignment of the CSA tensor within the molecular frame. This fundamental information about ^{19}F CSA tensors is not yet available for any fluorinated amino acid. Anisotropic values (but not the alignments) of ^{19}F chemical shift tensors have been reported for various systems including 5F-Trp, but not yet in the framework of any peptide or protein (Yim and Gilson, 1968; Mehring et al., 1971; Luck et al., 1996). For a few aromatic systems the respective principal tensor axes have been assigned to the molecular frame, but not yet for the indole ring of Trp (Snyder, 1965; Nehring and Saupe, 1970; Griffin et al., 1973; Halstead et al., 1975; Mehring 1983; Hiyama et al., 1986).

To first obtain the fundamental CSA parameters for 5F-Trp and then to tackle a biologically relevant question by ^{19}F-NMR, we have investigated here a particular structural aspect of the antimicrobial peptide gramicidin A (gA), which has attracted much attention over the past decade. The pentadecapeptide (HCO-Val-Gly-Ala-DLeu-Ala-DVal-Val-DVal-Trp-DLeu-Trp-DLeu-Trp-DLeu-Trp-NHCH$_2$CH$_2$OH) is known to form dimeric ion channels in membranes (Harold and Baarda, 1967; Arseniev et al., 1985; Killian, 1992). The rim of the right-handed β-helix is lined with four tryptophans, which play an important structural role in the membrane-immersion of the peptide (Killian, 1992; Hu et al., 1993; Pascal and Cross, 1993; Cotten et al., 1997) and which are functionally relevant for the conductivity and selectivity of the ion channel (Becker
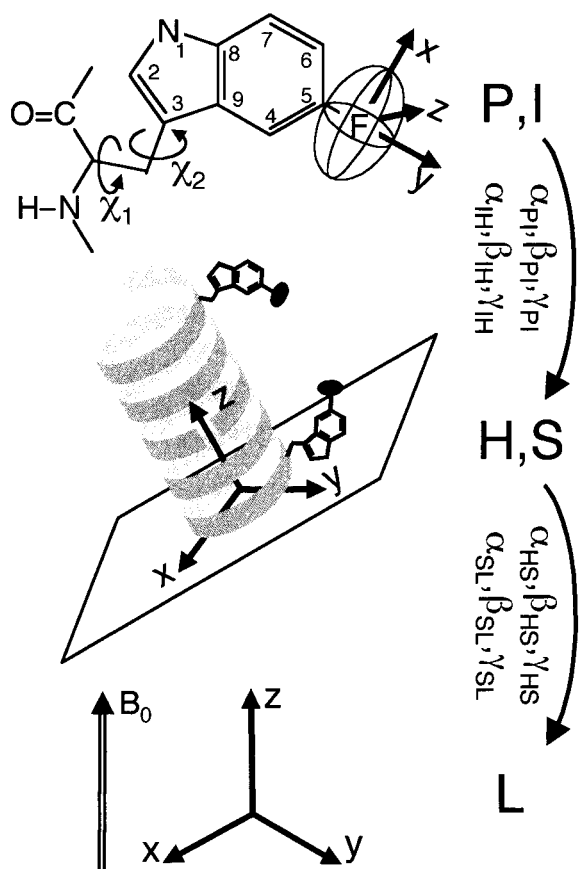
FIGURE 1 Alignment of the ^{19}F CSA tensor in the magnetic field B_0 is described by a series of Euler rotations of α, β, and γ, which are used to transform the tensor from one frame of reference to the next, namely from the principal axis system (P) to the indole ring system (I), to the helix axis system (H), to the macroscopically oriented sample (S), and finally to the laboratory frame (L).

et al., 1991; Hu and Cross, 1995; Hu et al., 1995; Busath et al., 1998). The structure of the peptide in liquid crystalline membranes has been fully resolved by previous ^{2}H-, ^{13}C-, and ^{15}N-NMR studies, revealing the detailed conformation and dynamics of the Trp side chains (Macdonald and Seelig, 1988; Ketchem et al., 1993, 1997; Koeppe et al., 1994, 2000; Cross et al., 1999). In recent functional studies of gA, ^{19}F-substituents were placed in various positions of the indole rings as a tool to modify their electric dipole moments, which provided valuable insights into the mechanism of ion transport (Anderson et al., 1998, 2001; Busath et al., 1998; Dorigo et al., 1999; Phillips et al., 1999; Thompson et al., 2001). Despite some appreciable electric dipole effects, the structural impact of the fluorine substitutions on the side chain torsion angles of Trp was found to be rather small, changing χ_1 by less than 5°, and χ_2 by less than 12° (Cotten 1998; Cotten et al., 1999) (for definitions of χ_1/χ_2, see Fig. 1). Given this reliable information on the structure of native gA and its ^{19}F-labeled analogues, here we have carried out the first direct ^{19}F-NMR analysis of 5F-Trp in a membrane-associated peptide. That way, it was not

only possible to establish the NMR approach and demonstrate its high sensitivity, but also to obtain new structural data on the side chain response in gA toward different phase states of the lipid bilayer.

MATERIALS AND METHODS

Samples

Three types of gramicidin A peptides were examined in this study: labeled at position 13 with 5F-Trp ["F13-gA"], at position 13 with 5F-(2,4,6,7)^{2}H-Trp ["F(d)13-gA"], or at position 15 with 5F-(2,4,6,7)^{2}H-Trp ["F(d)15-gA"]. See Fig. 1 for the numbering of the indole ring. The fluorinated peptides were synthesized by standard solid phase methods as described previously (Fields et al., 1988, 1989; Cotten et al., 1999). The peptides were incorporated in dimyristoylphosphatidylcholine (DMPC) purchased from Avanti Polar Lipids (Alabaster, AL) and used without further purification. Nonoriented powder samples of F(d)13-gA and F(d)15-gA were prepared by codissolving the peptide and DMPC at a peptide:lipid molar ratio of 1:10 in benzene with 5 vol% ethanol. The solvent was removed under vacuum, and the mixture was hydrated to 50% (weight/total weight) by adding high-performance liquid chromatography-grade water, as previously described (Cotten et al., 1999).

For the oriented samples, DMPC and gA at a 10:1 ratio (using either 9 mg F(d)13-gA, or 2 mg of F(d)15-gA or F13-gA) were cosolubilized in 450 μl of 95:5 vol/vol mixture of benzene/ethanol. The solution was distributed over 15 glass slides of 8 mm × 20 mm × 0.06-mm (Marienfeld, Lauda-Königshofen, Germany). After evaporating the solvent under N$_2$, the slides were dried under vacuum overnight. Samples containing F(d)13-gA and F(d)15-gA were hydrated to 50% by adding high-performance liquid chromatography-grade water to each slide with a micropipette and then stacked. The stack was covered with an additional slide, sealed with epoxide glue along the edges to prevent the sample from drying, and incubated for several days at 45°C. Alternatively, the glass slides with F13-gA were stacked first, then incubated at 98% humidity for 48 h until the sample became transparent, and finally wrapped in parafilm. Both approaches yielded equivalent results in terms of the peptide structure and mobility, although the latter sample had a significantly better mosaic spread.

Instrumentation

Solid-state ^{19}F-NMR spectra were acquired on a 500-MHz Varian Unity Inova spectrometer (^{19}F frequency at 470.3 MHz). A double-tuned (^{1}H/^{19}F) flat-coil probe (2.5 mm × 9 mm) from Doty Scientific (Columbia, SC) was used. The orientation of the flat coil could be adjusted with a goniometer to within 2°. The ^{19}F 90°-pulse length was 2.5 μs, and ^{1}H-decoupling of up to 40 kHz was applied. A Hahn echo with a 25-μs delay was used to acquire free induction decays of 5120 points (zero filled to 16,384) with a 2-μs dwell time over 10 ms. The recycle time was 3 to 4 s, and 5,000 to 10,000 scans were acquired, depending on the phase state and linewidth of the sample. A 100-Hz linebroadening was applied, and all chemical shift values were referenced with respect to CFCl$_3$ at 25°C. T$_2$-relaxation times were measured with an echo sequence over 10 suitably incremented delay times.

The degree of sample orientation was assessed by ^{31}P-NMR using a homebuilt flat-coil ^{1}H/X probe. In the first set of oriented samples containing F(d)13-gA and F(d)15-gA, ~50% of the material were well oriented, whereas the sample prepared later from F13-gA was oriented to 90%. An appropriate powder contribution was thus subtracted from the corresponding ^{19}F-NMR spectra, but this procedure had no impact on the analysis because the resulting lineshapes of analogous samples were very similar (despite the different amounts of powder contribution subtracted). The residual ^{19}F-background signal of the NMR probe was also subtracted.

Because most spectra contained a small signal of trifluoroacetic acid at -76 ppm, this narrow peak was replaced in the oriented spectra by a straight connection between -69 and -81 ppm to avoid any misfit in the lineshape simulations.

Lineshape simulations

The experimental ^{19}F spectra from oriented samples aligned at a tilt angle θ in the magnetic field were compared with lineshapes calculated numerically by a C^{2+} program. This strategy is illustrated in Fig. 1, where the chemical shift anisotropy tensor is successively rotated from one frame of reference to the next using three angles α, β, and γ each. The starting point in the lineshape simulations was the CSA tensor δ_P in the principal axis frame (P) for which the three principal axis values were obtained from the ^{19}F-NMR spectrum of lyophilized gA. First, the tensor was transferred via the indole ring frame (I) into the helix frame (H) with the z axis along the gA axis. Subsequently, the tensor was rotated into a sample frame (S) that is fixed with its z axis along the glass plate normal, as the helix axis may deviate from the sample normal due to "mosaic spread." Finally, the tensor was transferred into the laboratory frame (L) to account for the macroscopic sample tilt θ. The resulting resonance frequency is then given by the $(\delta_L)_{33}$-component of the tensor δ_L in the laboratory frame. For the complete spectrum, however, it has to be considered that the membrane environment defines only the gramicidin helix axis direction but not its azimuthal polarity. This, in addition to the mosaic spread, was taken into account by averaging over the three Euler angles α_{HS}, β_{HS}, and γ_{HS}, which transform the coordinate system H into S. The lineshapes were constructed from 10^6 randomly chosen Euler angle sets α_{HS}, β_{HS}, and γ_{HS} with uniformly distributed α_{HS} and γ_{HS}. The helix slant β_{HS} was varied according to a Gaussian distribution $p(\beta_{HS}) \sim \sin(\beta_{HS}) \exp[-\beta_{HS}^2/(2\sigma^2)]$ around $\beta_{HS} = 0$ with a standard deviation of $\sigma = 12°$, called the mosaic spread. Additional Lorentzian linebroadening of 1 to 2.5 kHz was applied to the simulated spectra to account for the intrinsic linewidth, choosing always the same value within any one tilt series.

Our discussion of the spatial relationship between the ^{19}F CSA tensor and tryptophan is based on the gramicidin A structure 1MAG.pdb, and on the indole geometry from the Sybyl database (Sybyl 6.4, Tripos Inc., St. Louis, MO), which is equivalent to the data used in the ^{2}H-NMR study of gA by Hu et al. (Hu and Cross, 1995; Hu et al., 1995). A different coordinate set for the Trp geometry had been used in the previous ^{2}H-NMR analysis on ^{19}F-substituted gA by Cotten et al. (Cotten, 1998; Cotten et al., 1999). Therefore, those ^{2}H-NMR data were re-evaluated here with the same indole geometry as Hu et al. to enable an unbiased comparison with our own ^{19}F-NMR data. It is important to realize that the precision at which the indole geometry can be derived from the literature or any database is rather limited and translates into an uncertainty of $\sim5°$ in the χ_1/χ_2 rotamer angles of the side chain.

Root of mean square deviation analysis

The spectral lineshapes of a tilt series were simulated from two different points of view, as there are two possible ways of describing the ^{19}F CSA tensor orientation with respect to the sample fixed frame (S). The first, ab initio approach makes use of two Euler angles α_{PS} and β_{PS}, which define the principal axis system of the CSA (P) with respect to the sample S. Alternatively, in the in situ approach, we start off with the known backbone structure of gramicidin A, and then the two rotamer angles χ_1 and χ_2 are used to describe the torsions around the Cα-Cβ and Cβ-Cγ bonds of Trp, respectively (for definition of χ_1 and χ_2, see International Union of Pure and Applied Chemistry and International Union of Biochemistry and Molecular Biology 1970). These two approaches are equivalent in defining the absolute CSA tensor orientation in S, and they can be readily interconverted, provided that the alignment of the tensor with respect to the indole geometry is known. Because this relationship has not yet been character-

ized for ^{19}F-labeled Trp, here we will deduce the CSA tensor alignment and axis assignment by comparing our ^{19}F-NMR ab initio data set with the previous ^{2}H-NMR in situ data set. For an unbiased representation of each set of NMR spectra, it is necessary to carry out a systematic conformational search and to validate the experimental data in an objective way. This was done by calculating the root mean square deviation (rmsd) between the simulated lineshapes and the experimental spectra of a complete tilt series, either as a function of α_{PS} and β_{PS} (ab initio), or as a function of χ_1 and χ_2 (in situ):

$$\text{rmsd} = \sqrt{\sum_i \sum_k (s_{\text{exp i,k}} - s_{\text{mod i,k}})^2/N}$$

Here, $s_{\text{exp i,k}}$ and $s_{\text{mod i,k}}$ are the amplitudes of the normalized experimental or model spectrum, respectively, where i denotes the sum over the different spectra obtained at different sample tilts in the magnetic field, k denotes the sum over all points of a spectrum, and N is the number of spectra within a tilt series.

Minima of the rmsd were calculated to obtain the best-fit ab initio tensor orientation and the best in situ side chain conformation, respectively. It should be noted that the combination of several lineshapes from a tilt series to yield a single rmsd value is not unproblematic, because there are various ways how their respective contributions could be weighted in view of their very different spectral widths. Nevertheless, we found that the rmsd minima obtained with a linear weighting procedure correspond to excellent fits of simulated and experimental lineshapes. Any other, more elaborate weighting models did not move the minima by more than 5°, hence our rmsd analysis leads to reliable results. Another potential source of error in the rmsd plots concerns the accuracy in the chemical shift determination, which is critical when the peak position in the 0° tilt spectrum lies close to the δ_{22} CSA tensor value, as it happens to be the case here. In this situation, an error of 1 ppm would translate into a shift of the rmsd minima of $\sim3°$ in β_{PS}, hence it is important to care about good referencing in the oriented samples (R. W. Glaser and A. S. Ulrich, submitted; R. Ulrich, R. W. Glaser, and A. S. Ulrich, submitted).

RESULTS

The anisotropy of the ^{19}F chemical shift is characterized by a tensor with the three principal values δ_{11}, δ_{22}, and δ_{33}. Our aim is to determine the two unique angles α and β, which describe the CSA alignment with respect to the lipid bilayer, as illustrated in Fig. 1. From these angles, we will then be able to deduce the conformation of the 5F-Trp side chain (i.e., χ_1 and χ_2 values) to which this CSA tensor is attached. First, we measure the three principal CSA values of 5F-Trp from nonoriented bilayer samples. Using aligned samples, contributions of [1]H-coupling, T_2-relaxation, and mosaic spread to the ^{19}F linewidth are assessed, and spectra of protonated and deuterated 5F-Trp samples are compared. Second, a tilted series of orientation-dependent spectra of uniaxially aligned samples is analyzed by lineshape simulation to determine the alignment of the ^{19}F CSA tensor with respect to the membrane. Next, we assign the three principal CSA axes with the aid of the known coordinates of gA. On this basis, we are able to position the CSA tensor into the molecular frame of the indole ring. Finally, the side chain conformation of Trp in the gel phase bilayer can be determined and compared with its alignment known from ^{2}H-NMR studies of the liquid crystalline phase. A special emphasis of this work concerns the behavior of gA in the
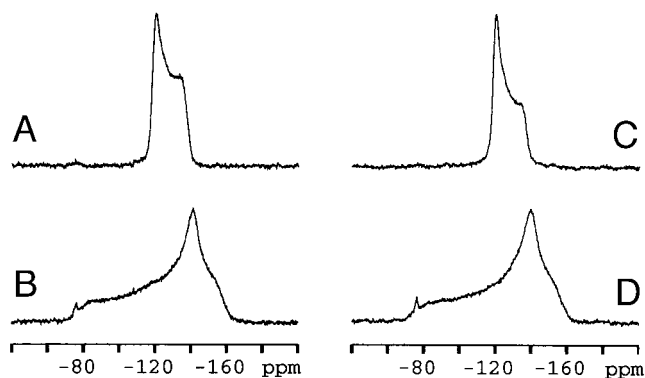
FIGURE 2 Solid-state ^{19}F-NMR powder spectra of gramicidin A labeled with 5F-Trp in either position 13 (*a* and *b*) or 15 (*c* and *d*), embedded in fully hydrated DMPC dispersions. At 35°C (*a* and *c*) the [1]H-decoupled powder spectra reflect an axially symmetric CSA tensor, which is motionally averaged by fast reorientation of the polypeptide about the membrane normal. This global motion ceases below the phase transition temperature (*b* and *d*), as nonaxially symmetric powder lineshapes are observed at 5°C, revealing the three principal values of the ^{19}F CSA tensor.

gel state of the membrane where the peptide is immobilized. Even though structural studies are rarely performed in the gel state (Scarlata, 1988, 1991; Takeuchi et al., 1990; Nicholson et al., 1991; Maruyama and Takeuchi, 1998), the general approach presented here will be relevant for any large membrane protein that does not undergo fast long-axial rotation in the lipid bilayer.

Powder samples

Fig. 2 shows the ^{19}F-NMR spectra for non-oriented samples of F(d)13-gA (*a*, *b*) and F(d)15-gA (*c*, *d*), incorporated into DMPC at a peptide:lipid ratio of 1:10. When acquired at 35°C, i.e., above the lipid phase transition temperature, the powder lineshapes (*a*, *c*) reflect axially symmetric CSA tensors. Both span the range from -120.0 ppm to -139.0 ppm, as estimated by a lineshape fitting procedure that takes linebroadening into account. This axial symmetry reflects the expected fast reorientation of the peptide about the membrane normal at 35°C (Macdonald and Seelig, 1988; Lee et al., 1993). Motional averaging, however, obscures the structural information contained in the anisotropy of the three distinct principal axes of the ^{19}F CSA tensor. Therefore, to apply the proposed NMR strategy to its full potential, it is important to prevent any global molecular rotation. The corresponding ^{19}F-NMR spectra at 5°C, where the peptide is immobilized in the gel phase of the lipid, are displayed in Fig. 2, *b* and *d*. These lineshapes now represent nonaxially symmetric CSA tensors, whose principal axis values δ_{11}, δ_{22}, and δ_{33} are extracted from the two edges and the maximum (Nicholson et al., 1991). Due to difficulties in chemical shift referencing in a flat-coil probe (R. W. Glaser and A. S. Ulrich, submitted; R. Ulrich, R. W. Glaser, and

A. S. Ulrich, submitted), absolute errors are on the order of ± 2 ppm, but the relative values are self-consistent within ± 1 ppm. For the label in position 13, the principal axis values are $\delta_{11} = -80.0$ ppm, $\delta_{22} = -141.5$ ppm, and $\delta_{33} = -156.5$ ppm, and for position 15 they are $\delta_{11} = -81.0$ ppm, $\delta_{22} = -141.0$ ppm, and $\delta_{33} = -157.5$ ppm. The isotropic chemical shifts are calculated to be $\delta_{iso} = -126.0$ for F(d)13-gA, and $\delta_{iso} = -126.5$ for F(d)15-gA, and the total width of both respective tensors is 76.5 ppm. The CSA width of the membrane-embedded peptide at 5°C is smaller than that of lyophilized gramicidin A ($\delta_{11} - \delta_{33} = 83$ ppm) and of polycrystalline 5F-Trp (87 ppm) (U. Dürr, S. L. Grage, and A. S. Ulrich, manuscript in preparation). This suggests that the gel phase lipid environment provides a limited degree of librational freedom for the Trp side chains, which are nevertheless subject to considerable intramolecular steric hindrance by neighboring amino acids (Nicholson et al., 1991; Koeppe et al., 2000). Upon cooling the polycrystalline amino acid down to -60°C, we observed a further increase in its CSA by ~ 10 ppm, approaching the rigid powder limit (data not shown). This trend compares well with the reported CSA widths of ^{15}N in the amide groups of gramicidin A from which the amplitudes of librational motion in the backbone have been estimated as ± 10° at -60°C and up to ± 20° in the lipid gel phase (Nicholson et al., 1991; Lazo et al., 1993, 1995). For the Trp side chains Hu et al. (1995) have reported librational amplitudes of ~ 30° in the liquid crystalline state. In the present study, however, all three ^{19}F CSA tensor values are affected by librational motion in a complex way, hence we do not attempt to attribute the observed averaging to any particular torsional axis nor to define an order parameter.

Oriented samples

When a uniaxially oriented sample is aligned horizontally, i.e., with its axis parallel to the static magnetic field direction ($\theta = 0$°), all labeled sites have the same orientation with respect to this direction. One specific frequency is selected from the powder spectrum, resulting in a single narrow peak. The ^{19}F-NMR spectra obtained this way from gA labeled in position 13 are shown in Fig. 3. The lineshapes are compared with and without [1]H-decoupling, both for protonated (*a*) and deuterated (*b*) 5F-Trp side chains, and each panel displays data for the two different temperatures of 35°C (liquid crystalline bilayer) and 5°C (gel phase). We note that the lipid phase transition has only a small effect on the resonance position (Fig. 3, *a* and *b*), suggesting that the Trp conformation is quite similar in both the fluid phase and the gel state environment. If the only consequence of lipid chain melting on gA were the onset of long-axial rotation, then the signal would remain exactly at the same frequency. However, there is a small but significant shift of 2.7 ppm toward the isotropic value in going from 5 to 35°C, which was confirmed by compiling [19]F-
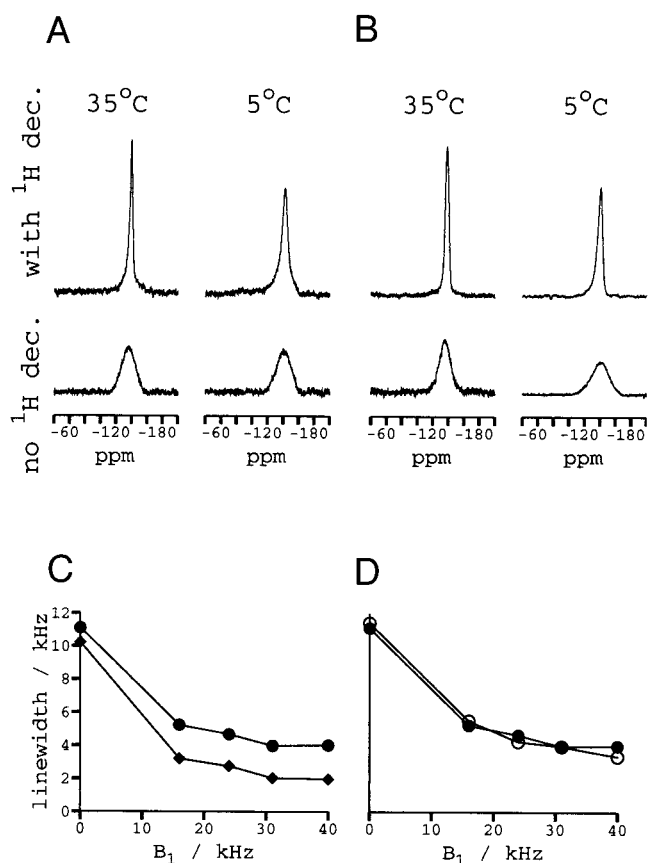
FIGURE 3 ^{19}F-NMR spectra (*a* and *b*) of macroscopically oriented samples with gA labeled in position 13 were acquired at temperatures above and below the lipid phase transition temperature, with and without [1]H-decoupling ($B_1 = 40$ kHz). The bottom two panels (*c* and *d*) depict the ^{19}F-NMR linewidths as a function of decoupling field strength. The two different temperatures (*c*) are compared, as well as nondeuterated and deuterated side chains (*d*) (●, protonated 5F-Trp at 5°C; ◆, protonated 5F-Trp at 35°C; ○, deuterated 5F-Trp at 5°C).

NMR data also from other oriented samples of gA (not shown). This small shift may thus be attributed to a slight local conformational change or to some additional motional averaging. It is likely that a slight wobble of the gA axis plus increased librational freedom of the Trp side chains is facilitated in the liquid crystalline phase of the lipid. In a simplistic approach, such motional averaging may be described by an isotropic order parameter S_{mol}. Its value can be estimated from the ratio of the observed CSA width of 19 ppm at 35°C (Fig. 2, *a* and *c*) over the theoretically expected CSA width {19 ppm + 3/2 × 2.7 ppm}, provided there is no conformational change. The resulting value of $S_{mol} \approx 0.8$ appears reasonable for the side chain of a transmembrane peptide, but it must only be regarded as a rough indicator of the extent of motional averaging. It will be shown below that the Trp torsion angles indeed respond slightly to the lipid phase state, hence it is not possible here to discriminate between motional effects and conformational changes.

The observed linewidths (at half height) of the oriented spectra are plotted in Fig. 3, *c* and *d* as a function of the [1]H-decoupling field strength B_1. Fig. 3 *c* illustrates the line-narrowing effect of motional averaging due to global peptide rotation in the liquid crystalline phase, and Fig. 3 *d* compares the linewidths of protonated and deuterated indole rings at 5°C. [1]H-decoupling is obviously essential for achieving optimal resolution. The nondecoupled linewidths of ~11 kHz start to decrease significantly when rather low decoupling power (20 kHz B_1 field strength) is applied. Above 40 kHz of [1]H-decoupling field strength, however, the residual ^{19}F-NMR linewidths of ~2 kHz in the fluid phase and 4 kHz in the gel state cannot be further improved. These large line widths cannot be attributed to transverse relaxation, because the measured T_2 relaxation times yield an intrinsic line width of $1/(\pi T_2) \approx 500$ Hz at 35°C, and $1/(\pi T_2) \approx 800$ Hz at 5°C, respectively. Likewise, we exclude susceptibility effects as a primary contribution, because in other ^{19}F-NMR studies of oriented samples we obtained line widths between 800 and 1500 Hz using the same setup (Salgado et al., 2002; R. W. Glaser and A. S. Ulrich, submitted). The dominant contribution to the considerable linewidths of gA in our samples stems from the orientational disorder of the peptide, which was estimated to be ~12° by lineshape simulation in both the gel state and the fluid phase. This large mosaic spread does not compare favorably with published data on gA aligned in liquid crystalline bilayers, where values as little as 0.3° have been reported (Hu and Cross, 1995; Hu et al., 1995). In fact, previous ^{2}H-NMR studies of the same ^{19}F-labeled compounds had also noted a significant increase in the orientational heterogeneity of the fluorinated side chains compared with the ^{19}F-free analogues (Cotten et al., 1999). Moreover, working in the gel phase seems to reduce the sample quality, as ^{15}N-NMR studies on gA at low temperature also encountered a significant linebroadening that could not be explained in terms of homogeneous relaxation broadening nor by a lack of [1]H-decoupling (Nicholson et al., 1991). It was argued that bilayer defects in the gel state are not annealed as well as in the liquid crystalline phase, which leads to a considerable range of helix orientations that are not motionally averaged.

The substitution of the indole protons by deuterons had no impact on the linewidth or the [1]H-decoupling efficiency in the gel state (Fig. 3 *d*). As the dipolar coupling to protons is usually a considerable source of linebroadening, this observation suggests strong intra- and intermolecular [1]H-^{19}F coupling to nearest neighbors. Additionally, the dipolar coupling between ^{19}F and the adjacent deuterons also has to be considered here, at least when working with low [1]H-decoupling strengths. Indeed [2]H-^{19}F dipolar splittings of up to 2 kHz have been observed by Cotten et al. (1999) on the same labeled samples, serving as a useful marker in assigning the ^{2}H-NMR resonances. At higher B_1 fields the effect of [1]H-decoupling on the linewidth diminishes in our system,
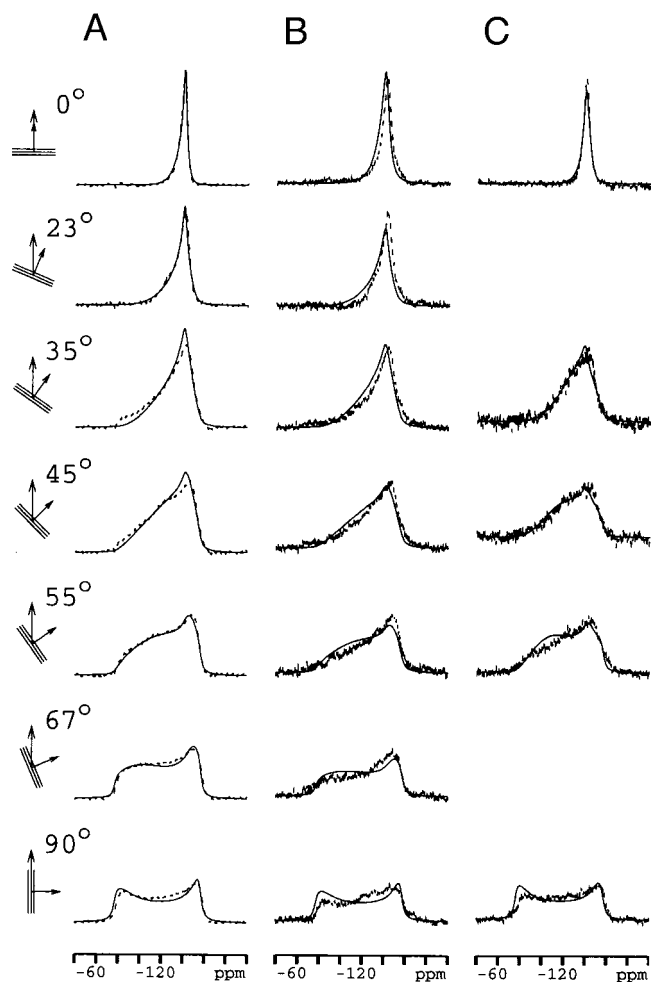
FIGURE 4 Experimental ^{19}F-NMR spectra (*dashed lines*) of F(d)13-gA (*a*), F13-gA (*b*), and F(d)15-gA (*c*). The macroscopically aligned membrane samples were tilted at an angle θ in the magnetic field, resulting in a set of lineshapes, which are characteristic of the CSA tensor orientation. Superimposed are the best-fit lineshape simulations (*solid lines*) corresponding to the minima in the respective rmsd plots of Fig. 5.

because the mosaic spread becomes the major contribution to the linebroadening. Our more recent experience with other ^{19}F-labeled compounds suggests that it may be advantageous to keep the neighboring protons, as otherwise simultaneous ^{1}H and ^{2}H decoupling would become necessary (U. Dürr, S. L. Grage, and A. S. Ulrich, manuscript in preparation).

Lineshape analysis

When an oriented gA sample was placed horizontally into the magnet ($\theta = 0°$), a single resonance line was observed, both at 35°C and 5°C (Fig. 3, *a* and *b*). Given the nonaxially symmetric CSA, the observed ^{19}F-NMR frequency is compatible with a manifold of different tensor orientations. When the peptides are immobilized in the gel phase, this

redundancy can be lifted by tilting the sample at an angle θ. As illustrated in Fig. 4, the ensemble of immobilized gA molecules, which differ in their azimuthal polarity, then gives rise to a distribution of ^{19}F-NMR frequencies. Tensor alignments that were indistinguishable at $\theta = 0°$ now become distinguishable by their characteristic ^{19}F-NMR lineshapes, and their Euler angles can be extracted by spectral simulation. In our first ab initio approach, we determine the relation between the CSA principal axis system (*P*) and a sample coordinate system (*S*) with the *z* axis pointing along the glass plate normal (see Fig. 1). The CSA orientation is described by two Euler angles α and β, whereas the third angle γ is evenly distributed about the sample normal. Fig. 5 shows the root mean square deviation (rmsd) between the experimental and calculated spectra, which were calculated in 1° increments for the entire orientational space spanned by α and β, for F(d)13-gA (left) and F(d)15-gA (right). Each plot combines the data from a complete series of tilt angles, as described in the Materials and Methods section. The rmsd plots possess several symmetries, corresponding to inherent redundancies in tensor alignment that cannot be lifted. When considering the symmetry properties of a nonaxially symmetric CSA tensor, there remains a fourfold ambiguity for $0° \; \alpha \; 180°$ and $0° \; \beta \; 180°$, which is correctly displayed in this analysis (Fig. 5).

The minima in the rmsd plots reflect those particular CSA tensor orientations relative to the bilayer normal that fit best to the experimental data. The corresponding angles are $\alpha = 80°/\beta = 79°$ (plus symmetry-related copies) for both F(d)13-gA and F13-gA and $\alpha = 90°/\beta = 73°$ (plus copies) for F(d)15-gA, within $\pm 5°$. Fig. 4 demonstrates an excellent agreement between the experimental ^{19}F-NMR spectra and the lineshape simulations obtained with the best-fit values of α and β for each individual gA sample investigated here. The protonated and deuterated Trp analogues in position 13 are fit by the same set of lineshapes, as expected, thus confirming the consistency and reproducibility of the sample preparation, the acquisition of tilt series, and the data analysis. Interestingly, the 5F-Trp spectra for positions 13 and 15 of gA resemble one another, which suggests that both indole rings must be aligned in a similar way. Previous ^{2}H-NMR studies of gA in the liquid crystalline state had indeed shown that all four Trp side chains assume a similar conformation (with the possible exception of Trp-9, about which there is still some disagreement in the literature) (Hu et al., 1993, 1995; Koeppe et al., 1994, 2000; Hu and Cross, 1995; Cotten et al., 1997; Cotten 1998). These indole orientations are functionally important as their electric dipole moments are aligned uniformly around the channel mouth to guide the entry of the ions.

CSA tensor assignment

So far, the CSA tensors have been successfully positioned with respect to the gel state lipid bilayer, but these results do
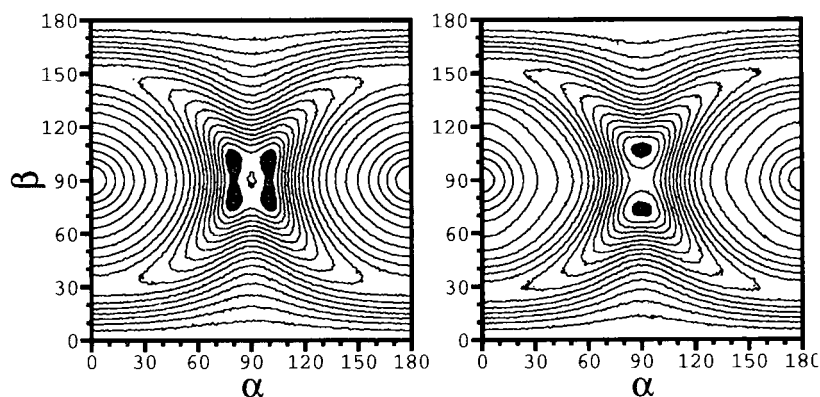
FIGURE 5   rmsd between the experimental ¹⁹F-NMR data from oriented samples at 5°C and the simulated lineshapes, where the Euler angles α and β relate the CSA principal axes to the axis of the sample. The analysis encompasses a complete series of spectra (see Fig. 4) acquired at different tilt angles of the sample in the magnetic field. The black areas show the rmsd minima at $\alpha = 80°$ and $\beta = 79°$ (plus symmetry related copies) for F(d)13-gA (*left panel*), and at $\alpha = 90°$ and $\beta = 73°$ (plus symmetric copies) for F(d)15-gA (*right panel*). Only the region $0° < \alpha < 180°$, $0° < \beta < 180°$ is depicted here, because the other quadrants are redundant due to symmetry.

not yet provide any information about the torsion angles χ_1 and χ_2 of the Trp side chains. To be able to draw such conclusions, the alignment of the CSA tensor has to be known with respect to the molecular frame of the indole ring. Such data is not available for 5F-Trp, but we will deduce this missing information from the previously reported structure of gA (Hu et al., 1993, 1995; Hu and Cross, 1995; Cotten et al., 1997; Cotten 1998). The published coordinates had been derived by ²H-NMR, using the very same gA peptides with ¹⁹F-labeled Trp side chains as in this ¹⁹F-NMR study. However, the previous ²H-NMR data had been acquired in DMPC bilayers at 40°C rather than in the lipid gel phase. Hence, we may use these coordinates on the assumption that the Trp side chain conformation is unaffected by the lipid phase transition, which is true to a first approximation (as outlined above, Fig. 3, *a* and *b*).

For the simulations of Figs. 4 and 5, the CSA tensor had not been constrained to the molecular scaffold of gA. As a next step we will now fix the principal axis of the CSA tensor with respect to the structure of gA that is known from the previous ²H-NMR studies. There are six straightforward and plausible possibilities to place the ¹⁹F CSA tensor into Trp: with one axis pointing along the C-F bond, another orthogonal axis lying in the indole plane, and the third axis being perpendicular to both. Lineshapes were simulated for the six possible permutations of the three axes, and the resulting spectral tilt series are summarized for F(d)13-gA in Fig. 6. The best agreement is seen in column 3, with the δ_{22} axis pointing along the C-F bond, δ_{11} lying in-plane of the indole ring, and δ_{33} aligned perpendicular. This axis assignment is in accordance with similar ¹⁹F CSA tensors that have been described in single crystal studies of fluorobenzenes and other fluorinated aromatic compounds (Snyder, 1965; Nehring and Saupe, 1970; Griffin et al., 1973; Halstead et al., 1975; Mehring, 1983; Hiyama et al., 1986).

DISCUSSION

The aim of this work was to introduce a new ¹⁹F-NMR strategy for structural studies in biomembranes, especially for peptides and proteins with tryptophan side chains. Incorporation of fluorotryptophan is a structurally conservative and highly sensitive approach to monitor directly any changes in the alignment and dynamics of the labeled side chain as well as the polypeptide on the whole. For example, the symmetry properties of the ¹⁹F-NMR powder lineshape readily reveal the onset of long-axial peptide rotation, when a membrane sample is heated through the lipid gel-to-liquid crystalline phase transition (see Fig. 2). For peptides that are immobilized in the gel state, we have demonstrated how the alignment of a ¹⁹F-labeled Trp side chain can be determined with respect to the membrane normal. The structure analysis of the indole ring is based on the anisotropic chemical shift of the ¹⁹F-label in a macroscopically oriented sample that has to be measured at different tilt angles. This approach was applied to gramicidin A labeled at position 13 or 15 with 5F-tryptophan that was either protonated or deuterated, - the latter being the same material that had been recently used in an analogous ²H-NMR study (Cotten et al., 1999). Based on the gA coordinates obtained by ²H-NMR in liquid crystalline DMPC, we were able to assign the principal axes of the ¹⁹F CSA tensor in the molecular frame of the 5F-Trp indole ring, notably in the same lipid environment but in the gel state. The most shielded CSA component δ_{33} of 5F-Trp was found to be perpendicular to the indole plane, δ_{22} to be aligned with the C-F bond, and the least shielded δ_{11} to be in-plane of the ring and orthogonal to the C-F bond.

To make the above tensor assignment, we had assumed that the principal axes of the CSA tensor are symmetrically constrained to the planar indole ring and to the C-F bond direction. The corresponding best fit of the predicted line-
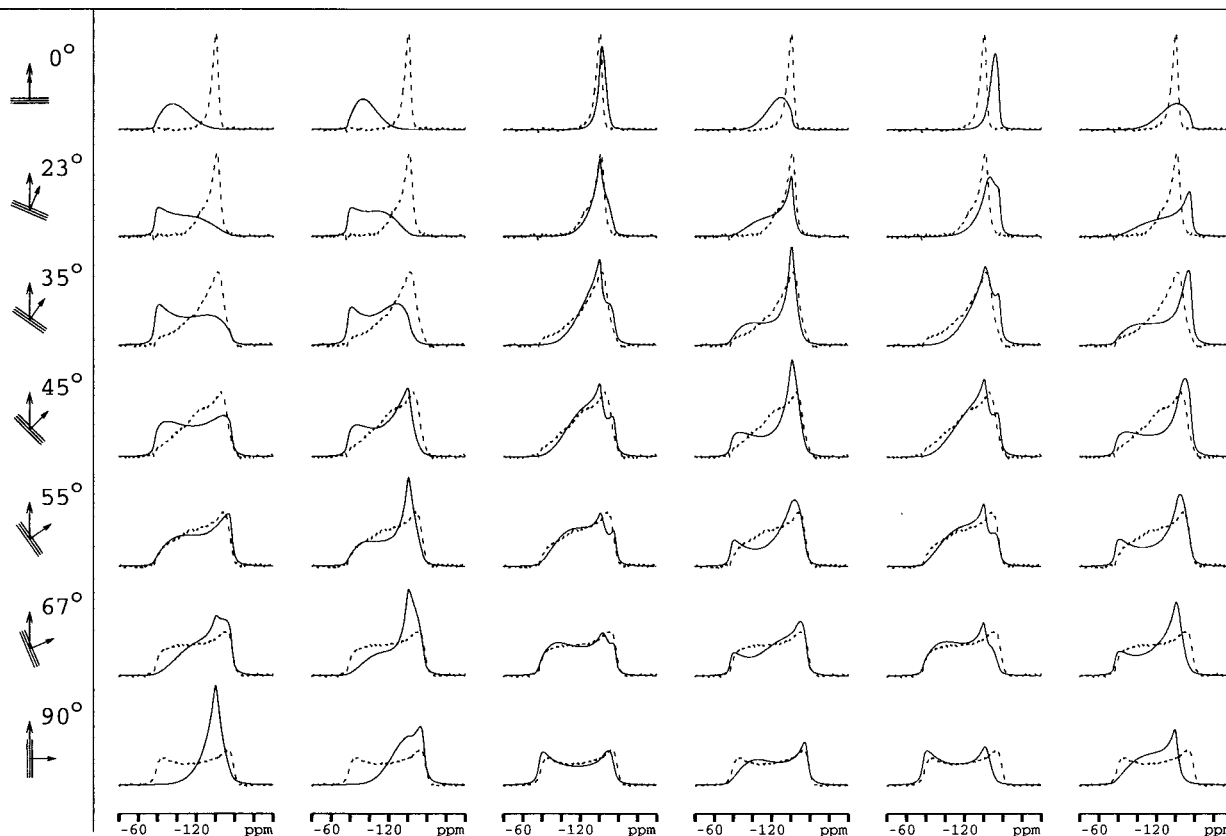
FIGURE 6 To assign the principal axes of the ^{19}F CSA tensor in the molecular frame of 5F-Trp, the six possible permutations were tested. The CSA coordinate system was constrained symmetrically to the indole ring with one of its principal axes aligned along the C-F bond, another axis perpendicular to the indole plane, and another axis within the plane. Based on the 5F-Trp side chain structure known from ^{2}H-NMR, the expected lineshapes for a uniaxially oriented sample at a series of tilt angles were calculated for the six possible assignments (*solid lines*). When compared with the experimental spectra of F(d)13-gA (*dashed lines*), only the assignment in column 3 gives a good fit, with δ_{22} parallel to the C-F bond, δ_{11} in the indole plane, and δ_{33} perpendicular to the ring.

shapes in Fig. 6 (column 3) does indeed reproduce all features of the experimental ^{19}F-NMR data quite well. However, the agreement is not as perfect as for the unconstrained case seen in Fig. 4, where the CSA tensor had been treated independently of any molecular framework. A possible explanation for this difference could be a deviation of the CSA principal axes from the ideal symmetry of the indole frame that had been assumed above. In that case the tensor would nonetheless be expected to obey the planar symmetry of the indole ring reasonably well, i.e., it should deviate mainly by a rotation around the indole normal. Allowing for such rotational deviation, however, it was not possible to find a tensor orientation that obeys the planar indole symmetry. Instead, we found that the δ_{33}-axis of our CSA tensor would have to be tilted away by ~20° from the indole normal.

The divergence was estimated by considering the Euler transformation (α_{PI}, β_{PI}, γ_{PI},) from the principal axis frame (P) to the indole-fixed frame (I, coinciding with P in the constrained case) the following way: We positioned the CSA tensor into the known framework of the gA molecule according to the Euler angles determined for the unconstrained case. Because the two systems P and I are indeterminate with regard to their rotation about the sample normal, their azimuthal difference $\Delta\gamma = \gamma_{PS} - \gamma_{IS}$ and hence the Euler angles α_{PI}, β_{PI}, γ_{PI} are not uniquely defined. An additional assumption is necessary to closer specify the tensor orientation in the indole-fixed frame. It is reasonable to choose the remaining free parameter $\Delta\gamma$ such that the planar indole symmetry is most fully conserved, i.e., the z axis of P is closest to the z axis of I. This is the case for $\Delta\gamma = 0°$ (or 180°), yielding $\alpha_{PI} = 80°$, $\beta_{PI} = 19°$, $\gamma_{PI} =$
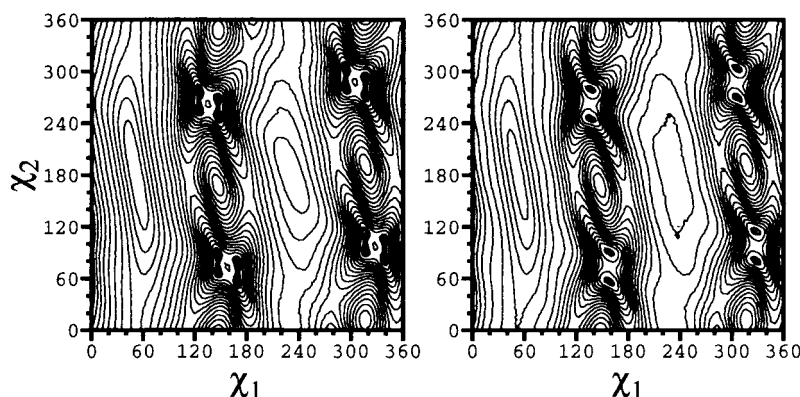
FIGURE 7   Using the fundamental assignment of the ^{19}F CSA tensor axes (see Fig. 6), the conformation of the 5F-Trp side chains in gA can now be refined in terms of the two torsion angles χ_1 (Cα-Cβ bond) and χ_2 (Cβ-Cγ bond). In analogy to Fig. 5, rmsd plots were generated for F(d)13-gA (*left panel*) and F(d)15-gA (*right panel*) as a function of χ_1 and χ_2. The minima display the allowed conformations of the two 5F-Trp side chains on gA in the gel state of the lipid membrane, as summarized in Table 1. The full range from $0° < \chi_1 < 360°$, $0° < \chi_2 < 360°$ is depicted here, as the angles are unique because of their relation to the peptide backbone.

$-87°$ (plus three further, equivalent solutions). The transformation described by these Euler angles is close to a rotation of β_{PI} about the *x* axis, which would be $\alpha_{PI} = 90°$, β_{PI}, $\gamma_{PI} = -90°$). That way, we estimated that the tensor's δ_{33}-axis is tilted away from the indole normal by ~20°, hence it does not obey the planar symmetry of the aromatic ring.

There may be two explanations to account for this apparent discrepancy between the CSA alignment obtained here ab initio by ^{19}F-NMR on the one hand and the predicted CSA alignment on the other hand that had been calculated under the assumption that the tensor is fixed to the molecular coordinates of gA known from ^{2}H-NMR. First, the ^{19}F CSA tensor could indeed be significantly tilted out-of-plane of the indole ring due to the influence of neighboring side chains, the lipid environment, or hydrogen-bonds formed. However, as the CSA tensor orientation is usually a rather local property of the environment, a CSA tensor not obeying the planar indole symmetry seems rather implausible. The few ^{19}F CSA tensor alignments that are known for aromatic crystalline compounds, where the impact of neighboring groups is just as likely as in gA, show only small deviations of a few degrees (Snyder, 1965; Nehring and Saupe, 1970; Griffin et al., 1973; Halstead et al., 1975; Mehring, 1983; Hiyama et al., 1986). As an alternative explanation we therefore propose that the side chain conformation measured here at 5°C differs from the conformation described previously by ^{2}H-NMR at 40°C. After all, the previous 5F-Trp coordinates had been obtained in a liquid crystalline lipid environment, and they were used only to a first approximation for the current analysis of gA in the gel phase (Hu et al., 1993, 1995; Hu and Cross, 1995; Cotten et al., 1997; Cotten, 1998).

Given the arguments above, we attribute the slight but significant mismatch of the experimental and simulated spectra in Fig. 6 (column 3) to genuine differences in the side chain conformation in the different phase states of the lipid bilayer. Hence, by an in situ analysis of the 5F-Trp alignment, it is possible now to determine directly the torsion angles χ_1 and χ_2 in the gel phase. The side chain conformation was structurally refined under the following two assumptions: 1) The Cα-Cβ orientation stays the same below and above the phase transition temperature, meaning that the structure of the hydrogen-bonded gA backbone does not change; and 2) the CSA tensor is aligned with its axes pointing along the indole-fixed frame directions according to the assignment of Fig. 6 (column 3). The in situ rmsd analysis for F(d)13-gA as a function of the two rotamer angles χ_1 and χ_2 is shown in Fig. 7. This plot is basically a translation from the general orientational space spanned by the Euler angles α and β (as in Fig. 5) into the conformational space of χ_1 and χ_2, leaving out those orientations that are not sterically accessible by any combination of torsion angles. Each of the four sets of minima in the χ_1/χ_2 map correspond precisely to the minima found in the α-β map, meaning that the ab initio 5F-Trp orientations are indeed readily accessible by rotations about the Cα-Cβ and Cβ-Cγ bonds of the peptide. It is not yet possible to tell from the ^{19}F-NMR data alone, which of the symmetry-related solutions corresponds to the actual side chain conformation in gA, just as the previous ^{2}H-NMR studies had to leave this question open. Table 1 summarizes the most reasonable group of solutions in analogy to the ^{2}H-NMR results. Studies are currently in progress to find the unique solution from [19]F-^{19}F dipolar distance constraints between two ^{19}F-labeled indole rings.

When comparing the values of χ_1 and χ_2 in Table 1 for the liquid crystalline phase and the gel state, the differences of ~10° to 20° suggest a small but significant change in the conformation of both Trp-13 and -15 upon passing through the lipid phase transition. (This does not however jeopardize the fundamental assignment of the CSA tensor axes in Fig.

TABLE 1 Possible side chain torsion angles of 5F-Trp in positions 13 and 15 of gA embedded in DMPC, listed pairwise as a combination of χ_1/χ_2 with an error of ±5°

F(d)13-gA	
Gel state (^{19}F-NMR at 5°C)	Liquid crystalline (^{2}H-NMR at 40°C)
294 (291)/281 (278)	304 (300)/257 (263)
294 (290)/304 (302)	304 (297)/318 (315)
316 (314)/272 (270)	
316 (312)/293 (292)	
F(d)15-gA	
Gel state (^{19}F-NMR at 5°C)	Liquid crystalline (^{2}H-NMR at 40°C)
306 (306)/271 (273)	295 (294)/284*(274)
307 (304)/303 (307)	295 (292)/300* (301)

*Minima not clearly resolved.
Several symmetry-related solutions were obtained (see Fig. 7) that cannot be distinguished from the orientational NMR constraints alone. The ^{19}F-NMR data were measured at 5°C (Fig. 7), whereas ^{2}H-NMR had been performed at 40°C above the lipid phase transition. The original ^{2}H-NMR data of Cotten et al. are reevaluated here to be compatible with the indole geometry taken from the Sybyl database (as used by Hu et al. 1995). To illustrate the intrinsic error associated with the choice of coordinates, the χ_1/χ_2 values in parenthesis are stated as equivalent solutions that are obtained when the Trp coordinates are taken from the pdb file 1MAG.pdb instead (as used by Cotten, 1998 and Cotten et al., 1999).

6). It is indeed reasonable to suppose that the peptide side chains will respond to the considerable increase in bilayer thickness in the gel state, especially as the Trp residues are located in the hydrophilic-hydrophobic interface of the membrane. In view of the multiple allowed solutions, it is not yet possible to recognize any systematic kind of orientational change, such as an adjustment toward an ideal *trans/gauche* conformation, or toward a more parallel alignment of the indole ring with the lipid chains. To systematically assess the effect of bilayer thickness it would now be interesting to monitor the Trp behavior in various lipids with different acyl chain lengths. Because the indole dipole orientations play a significant role in the function of the gramicidin A ion channel, previous studies in membrane-mimicking environments have also paid close attention to the conformation of the tryptophan side chains (Arseniev et al., 1985; Ketchem et al., 1997; Townsley et al., 2001). A comparison of the solid-state NMR structure in planar bilayers with solution state ^{1}H-NMR results in micelles revealed differences in torsion angles on the same order of magnitude as those detected here for the change in the lipid phase state. Because ^{19}F-labeling itself induces a slight conformational change of similar size, however, it is not meaningful to compare these χ_1/χ_2 values further.

With regard to the accuracy of the proposed values, it is important to point out that different choices of published indole coordinates lead to an intrinsic uncertainty of ~5° in determining the Trp conformation. Hence, our results are accurate to within 10°, given the quality of fit between the experimental ^{19}F-NMR data and the simulated lineshapes. The values in Table 1 illustrate the influence of choosing a particular set of indole geometries, namely those used by Hu et al. (Hu and Cross, 1995; Hu et al., 1995) and used throughout this publication or by Cotten et al. (Cotten et al., 1997; Cotten, 1998). As noted in the Materials and Methods section, the indole geometries found in the literature and in databases differ only very slightly among each other, but these small differences translate into variations in χ_1 and χ_2 of ~5°. Nonetheless, even if we had based our entire analysis on the indole geometry used by Cotten et al. (Cotten et al., 1997; Cotten, 1998), this would only have marginally altered the simulated lineshapes on which the tensor axes assignment is based here, leaving our fundamental assignment and other basic conclusions unchanged. We also note that our ^{19}F-NMR analysis of the single nonaxially symmetric CSA tensor has yielded 4×4 minima in the full range between 0° and 360° (e.g., for F(d)13-gA), whereas only 4×2 minima were observed in previous ^{2}H-NMR studies. This finding is consistent with the inherently higher symmetry of the single ^{19}F CSA tensor compared with two or more magnetically inequivalent ^{2}H-labels on an indole ring, yielding a higher information content for the latter case. Furthermore, in contrast to the ^{2}H-NMR study by Cotten et al. (Cotten et al., 1999), all minima in our χ_1/χ_2 plots have the same rmsd value. This means that all of the best-fit conformations in our unconstrained α/β space are just as readily accessible in the constrained χ_1/χ_2 space. Differences in the depths of the minima would be observed in cases where only a subset of the absolute minima in α/β space were accessible in the χ_1/χ_2 space.

The strategy of labeling with ^{19}F allowed for highly sensitive NMR experiments, requiring only small amounts of material, such as 2 mg peptide. Typical acquisition times were between 4 and 10 h, depending on the spectral lineshape to be measured (narrow peaks for horizontally oriented samples, or wideline spectra from tilted samples). These experimental ^{19}F-NMR conditions call for a direct comparison with previous ^{2}H- and ^{15}N-NMR studies on similar gA samples. For example, Cotten et al. (Cotten et al., 1997; Cotten 1998) used ~25 mg of the same ^{19}F/^{2}H-labeled peptide to obtain oriented ^{2}H-NMR spectra in 6 h. Koeppe et al. (1994, 1995, 2000) have also studied ^{2}H-labeled Trp in gA and used 6 mg (or 12 mg) peptide to acquire spectra over a period of 1 to 3 days (or 12–36 h, respectively), and a related study on ^{2}H-labeled valine in gA needed 50 mg to obtain powder spectra in 8 h (Lee et al., 1995). Previous ^{15}N-NMR studies required 1 to 2.5 days (and up to 4 days) to obtain powder-lineshapes with 80 mg of peptide (Hu et al., 1993, 1995; Hu and Cross, 1995). Given that the intrinsic sensitivity of an NMR experiment scales with the gyromagnetic ratio as $\gamma^{5/2}$ (Ernst et al., 1990; Abragam, 1996), ^{19}F theoretically offers a 100-fold advantage in sensitivity compared with ^{2}H, and 1000-fold compared with ^{15}N. This translates into an even greater reduc-

tion in measurement time if the same amount of material was to be used (since S/N $\propto \sqrt{\text{time}}$). However, these factors are reduced by approximately one order of magnitude, because, in the case of ^{2}H-NMR, the faster T_1-relaxation allows shorter recycle delays. Likewise, cross-polarization from ^{1}H improves the situation for ^{15}N-NMR by a factor of 10 (γ_H/γ_N). Furthermore, our ^{19}F-NMR spectra suffer from a much higher mosaic spread in the lipid gel phase than what is usually encountered in liquid crystalline membranes. The resulting line broadening appears to be the main reason why the sensitivity of analogous ^{2}H-NMR studies on gramicidin A in the gel phase has been prohibitively low. A related disadvantage of our static ^{19}F-NMR analysis is the necessity to acquire wideline spectra of tilted samples, however, this situation may be improved by MAOSS spectroscopy (Glaubitz and Watts, 1998; Glaubitz et al., 1999, 2000). Other important factors in assessing the sensitivity, such as the Q-factor of the NMR probe, cannot be evaluated here, except for stating that the previous NMR studies were carried out on 300 to 600 MHz spectrometers, while we used a 500-MHz instrument. Overall, we conclude that the effective gain in sensitivity achieved by ^{19}F-NMR offers at least a 10-fold reduction in material compared with ^{2}H-NMR, and 100-fold compared with ^{15}N-NMR, based on the direct comparison with previous studies on the very same peptide.

As a fundamental aspect in assessing the advantages and disadvantages of either labeling strategy, we note that the ^{19}F-NMR approach requires immobilization of the molecules to be able to acquire and interpret a tilt series of wideline spectra. In our case immobilization was achieved by working in the gel phase, but the same condition will apply to large membrane proteins that do not undergo fast long-axial rotation in a liquid crystalline bilayer. For such an immobilized sample the ^{19}F-NMR approach then provides two Euler angles from a single ^{19}F-label. To yield a comparable information content, ^{2}H-NMR requires at least two nonsymmetry-related labels at different sites. The major criticism of ^{19}F-labeling obviously concerns any potential modifications in the protein structure or function. For the case of 5F-Trp in gA the resulting differences in side chain torsion angles were found to be less than 5° in χ_1 and less than 12° in χ_2, which is significant but not dramatic (Cotten et al., 1999). Given the remarkable sensitivity gain, ^{19}F-labeling could become the method of choice when the material, the acquisition time, or the NMR coil-size is limited. This may be relevant in the case of large membrane proteins or recombinant material (which can be biosynthetically labeled with 5F-Trp), or when high lipid-to-peptide ratios are necessary to prevent aggregation (R. W. Glaser and A. S. Ulrich, submitted). Having shown that it is feasible to monitor the conformational response of 5F-Trp toward changes in the lipid environment, and having determined the fundamental ^{19}F-NMR parameters, it is now possible to further investigate the role of tryptophan as a membrane anchor and as an ion channel modulator in other proteins.

CONCLUSIONS

A difference of ~20° in the indole alignment of Trp was observed between our current data obtained in the lipid gel state and the previously reported gA coordinates in the fluid phase. The most likely explanation for this difference is a slight change in the Trp side chain conformation upon lipid chain melting when the bilayer thickness decreases significantly. On the assumption that the CSA tensor is symmetrically related to the indole geometry, we propose a distinct set of side chain torsion angles for 5F-Trp in positions 13 and 15 below the phase transition, which differ by 10° to 20° from those in the fluid phase. The overall features of the indole alignment, nevertheless, are quite similar in either lipid phase: the indole plane is aligned approximately parallel with the lipid acyl chains, and the C-F bond is pointing roughly along the membrane normal.

REFERENCES

Abragam, A. 1996. Principles of Nuclear Magnetism. Clarendon Press, Oxford, UK.

Anderson, D. G., R. B. Shirts, T. A. Cross, and D. Busath. 2001. Noncontact dipole effects on channel permeation: V. Computed potentials for fluorinated gramicidin. *Biophys. J.* 81:1255–1264.

Anderson, O. S., D. V. Greathouse, L. L. Providence, M. D. Becker, and R. E. Koeppe II. 1998. Importance of tryptophan dipoles for protein function: 5-fluorination of tryptophans in gramicidin A channels. *J. Am. Chem. Soc.* 120:5142–5146.

Arseniev, A. S., I. L. Barsukov, V. F. Bystrov, A. L. Lomize, and A. Ovchinnikov Yu. 1985. ^{1}H-NMR study of gramicidin A transmembrane ion channel: head-to-head right-handed, single-stranded helices. *FEBS Lett.* 186:168–174.

Asakura, T., M. Minami, R. Shimada, M. Demura, M. Osanai, T. Fujito, M. Imanari, and A. S. Ulrich. 1997. [2]H-labeling of Bombyx mori silk fibers and their structural characterization by solid state ^{2}H-NMR. *Macromolecules.* 30:2429–2435.

Avdonin, V., and T. Hoshi. 2001. Modification of voltage-dependent gating of potassium channels by free form of tryptophan side chain. *Biophys. J.* 81:97–106.

Becker, M. D., D. V. Greathouse, R. E. Koeppe, I. I., and O. S. Andersen. 1991. Amino acid sequence modulation of gramicidin channel function: effects of tryptophan-to-phenylalanine substitution on the single-channel conductance and duration. *Biochemistry.* 30:8830–8839.

Bouchard, M., C. Paré, J. P. Dutasta, J. P. Chauvet, C. Gicquaud, and M. Auger. 1998. Interaction between G-Actin and various types of liposomes: A ^{19}F, ^{31}P, and ^{2}H nuclear magnetic resonance study. *Biochemistry.* 37:3149–3155.

Busath, D. D., C. D. Thulin, R. W. Hendershot, L. R. Phillips, P. Maughan, C. D. Cole, N. C. Bingham, S. Morrison, L. C. Baird, R. J. Hendershot, M. Cotten, and T. A. Cross. 1998. Noncontact dipole effects on channel

permeation: I. Experiments with (5F-indole)Trp13 gramicidin A channels. *Biophys. J.* 75:2830–2844.

Clayton, A., and W. H. Sawyer. 1999a. The structure and orientation of class-A amphipathic peptides on a phospholipid bilayer surface. *Eur. Biophys. J.* 28:133–141.

Clayton, A. H. A., and W. H. Sawyer. 1999b. Tryptophan rotamer distributions in amphipathic peptides at a lipid surface. *Biophys. J.* 76: 3235–3242.

Cotten, M. 1998. Solid state NMR studies of gramicidin A. Ph.D. thesis. Tallahassee, Florida State University.

Cotten, M., C. Tian, D. D. Busath, R. B. Shirts, and T. A. Cross. 1999. Modulating dipoles for structure-function correlations in the gramicidin A channel. *Biochemistry.* 38:9185–9197.

Cotten, M., F. Xu, and T. A. Cross. 1997. Protein stability and conformational rearrangements in lipid bilayers: linear gramicidin, a model system. *Biophys. J.* 73:614–623.

Cross, T. A., F. Tian, M. Cotten, J. Wang, F. Kovacs, and R. Fu. 1999. Correlation of structure, dynamics and function in the gramicidin channel by solid-state NMR spectroscopy: gramicidin and related ion channel-forming peptides. Novartis Foundation Symposium 225, Chichester, Wiley, 225:4–22.

Danielson, M. A., and J. J. Falke. 1996. Use of ^{19}F NMR to probe protein structure and conformational changes. *Annu. Rev. Biophys. Biomol. Struct.* 25:163–195.

de Planque, M. R., D. V. Greathouse, R. E. Koeppe 2nd, H. Schafer, D. Marsh, and J. A. Killian. 1998. Influence of lipid/peptide hydrophobic mismatch on the thickness of diacylphosphatidylcholine bilayers: a ^{2}H NMR and ESR study using designed transmembrane α-helical peptides and gramicidin A. *Biochemistry.* 37:9333–9345.

Demura, M., Y. Yamazaki, T. Asakura, and K. Ogawa. 1998. Structure of uniaxially aligned ^{13}C labeled silk fibroin fibers with solid state ^{13}C NMR. *J. Mol. Struct.* 441:155–163.

Dorigo, A. E., D. G. Anderson, and D. D. Busath. 1999. Noncontact dipole effects on channel permeation: II. Trp conformations and dipole potentials in gramicidin A. *Biophys. J.* 76:1897–1908.

Ernst, R. R., G. Bodenhausen, and A. Wokaun. 1990. Principles of Nuclear Magnetic Resonance in One and Two Dimensions. Clarendon Press, Oxford.

Feeney, J., J. E. McCormick, C. J. Bauer, B. Birdsall, C. M. Moody, B. A. Starkmann, D. Y. Young, P. Francis, R. H. Havlin, W. D. Arnold, and E. Oldfield. 1996. ^{19}F nuclear magnetic resonance chemical shifts of fluorine containing aliphatic amino acids in protein: studies on lactobacillus casei dihydrofolate reductase containing (2S, 4S)-5-fluoroleucine. *J. Am. Chem. Soc.* 118:8700–8706.

Fields, C. G., G. B. Fields, R. L. Noble, and T. A. Cross. 1989. Solid phase peptide synthesis of ^{15}N-gramicidins A, B, and C and high performance liquid chromatographic purification. *Int. J. Peptide Protein Res.* 33: 298–303.

Fields, G. B., C. G. Fields, J. Petefish, H. E. V. Wart, and T. A. Cross. 1988. Solid-phase peptide synthesis and solid-state NMR spectroscopy of [Ala3–^{15}N][Val1]gramicidin A. *Proc. Natl. Acad. Sci. U. S. A.* 85: 1384–1388.

Friedrich, C. L., A. Rozek, A. Patrzykat, and R. E. Hancock. 2001. Structure and mechanism of action of an indolicidin peptide derivative with improved activity against gram-positive bacteria. *J. Biol. Chem.* 276:24015–24022.

Fu, R., and T. A. Cross. 1999. Solid-state nuclear magnetic resonance investigation of protein and peptide structure. *Annu. Rev. Biophys. Biomol. Struct.* 28:235–268.

Gerig, J. T. 1994. Fluorine NMR of proteins. *Prog. N.M.R. Spec.* 26: 293–370.

Gerig, J. T. 1998. Fluorine NMR. Biophysics textbook on-line, NMR section, chapter 24. www.biosci.umn.edu/biophys/OTLB/ NMR.html#24. Bloomfield, V.

Glaubitz, C., I. J. Burnett, G. Gröbner, A. J. Mason, and A. Watts. 1999. Deuterium-MAS NMR spectroscopy on oriented membrane proteins: applications to photointermediates. *J. Am. Chem. Soc.* 121:5787–5794.

Glaubitz, C., M. Carravetta, M. Eden, and M. H. Levitt. 2000. Toward dipolar recoupling in macroscopically ordered samples of membane proteins rotating at the magic angle. *Future Biol. Solid State N.M.R,* 4:10.–8.10.2000.

Glaubitz, C., and A. Watts. 1998. Magic angle-oriented sample spinning (MAOSS): a new approach toward biomembrane studies. *J. Magn. Reson.* 130:305–316.

Goetz, J. M., B. Poliks, D. R. Studelska, M. Fischer, K. Kegelbrey, A. Bacher, M. Cushman, and J. Schaefer. 1999. Investigation of the binding of fluorolumazines to the 1-MDa capsid of lumazine synthase by ^{15}N{^{19}F} REDOR NMR. *J. Am. Chem. Soc.* 121:7500–7508.

Grage, S. L., J. Salgado, U. Dürr, S. Afonin, R. W. Glaser, and A. S. Ulrich. 2001. Solid state ^{19}F-NMR of biomembranes. *In* Perspectives on Solid State NMR in Biology. S. R. Kiihne and H. J. M. deGroot, editors. Kluwer Academic Publishers, London. 83–91.

Griffin, R. G., H.-N. Yeung, M. D. LaPrade, and J. S. Waugh. 1973. Fluorine chemical shielding tensors and crystal structure of potassium tetrafluorophthalate. *J. Chem. Phys.* 59:777–783.

Halstead, T. K., H. W. Spiess, and U. Haeberlen. 1975. ^{19}F and ^{1}H shielding tensors and crystal structure of 4,4′-difluorobiphenyl. *Mol. Phys.* 31:1569–1583.

Hancock, R. E., and G. Diamond. 2000. The role of cationic antimicrobial peptides in innate host defences. *Trends Microbiol.* 8:402–410.

Harold, F. M., and J. R. Baarda. 1967. Gramicidin, valinomycin, and cation permeability of streptococcus faecalis. *J. Bacteriol.* 94:53–60.

Hiyama, Y., J. V. Silverton, D. A. Torchia, J. T. Gerig, and S. J. Hammond. 1986. Molecular structure and dynamics of crystalline *p*-fluoro-D, L-phenylalanine: a combined X-ray/NMR investigation. *J. Am. Chem. Soc.* 108:2715–2723.

Hofmann, A., C. Raguenes-Nicol, B. Favier-Perron, J. Mesonero, R. Huber, F. Russo-Marie, and A. Lewit-Bentley. 2000. The annexin A3-membrane interaction is modulated by an N-terminal tryptophan. *Biochemistry.* 39:7712–7721.

Hu, W., and T. A. Cross. 1995. Tryptophan hydrogen bonding and electric dipole moments: functional roles in the gramicidin channel and implications for membrane proteins. *Biochemistry.* 34:14147–14155.

Hu, W., N. D. Lazo, and T. A. Cross. 1995. Tryptophan dynamics and structural refinement in a lipid bilayer environment: solid state NMR of the gramicidin channel. *Biochemistry.* 34:14138–14146.

Hu, W., K. C. Lee, and T. A. Cross. 1993. Tryptophans in membrane proteins: indole ring orientations and functional implications in the gramicidin channel. *Biochemistry.* 32:7035–7047.

Jude, A. R., D. V. Greathouse, M. C. Leister, and R. E. Koeppe 2nd. 1999. Steric interactions of valines 1, 5, and 7 in gramicidin A channels. *Biophys. J.* 77:1927–1935.

Kameda, T., Y. Ohkawa, K. Yoshizawa, J. Naito, A. S. Ulrich, and T. Asakura. 1999a. Hydrogen-bonding in serine side-chains of *Bombyx mori* and *Samia cynthia ricini* silk fibroins using solid state ^{2}H-NMR. *Macromol.* 32:7166–7171.

Kameda, T., Y. Ohkawa, K. Yoshizawa, E. Nakano, A. S. Ulrich, and T. Asakura. 1999b. Dynamics of the tyrosine side-chains of *Bombyx mori* and *Samia ricini* silk fibroins using solid state ^{2}H-NMR. *Macromol.* 32:8491–8495.

Keniry, M. A., A. Kintanar, R. L. Smith, H. S. Gutowsky, and E. Oldfield. 1984. Nuclear magnetic resonance studies of amino acids and proteins: deuterium nuclear magnetic resonance relaxation of deuteriomethyl-labeled amino acids in crystals and in *Halobacterium halobium* and *Escherichia coli* cell membranes. *Biochemistry.* 23:288–298.

Ketchem, R. R., W. Hu, and T. A. Cross. 1993. High-resolution conformation of gramicidin A in a lipid bilayer by solid-state NMR. *Science.* 261:1457–1460.

Ketchem, R. R., B. Roux, and T. A. Cross. 1997. High-resolution polypeptide structure in a lamellar phase lipid environment from solid state NMR derived orientational constraints. *Structure.* 5:1655–1669.

Killian, J. A. 1992. Gramicidin and gramicidin-lipid interactions. *Biochem. Biophys. Acta.* 1113:391–425.

Klug, C. A., K. Tasaki, N. Tjandra, C. Ho, and J. Schaefer. 1997. Closed form of liganded glutamine-binding protein by rotational-echo double-resonance NMR. *Biochemistry.* 36:9405–9408.

Koenig, B. W., J. A. Ferretti, and K. Gawrisch. 1999. Site-specific deuterium order parameters and membrane-bound behavior of a peptide fragment from the intracellular domain of HIV-1 gp41. *Biochemistry.* 38:6327–6334.

Koeppe II, R. E., J. Hatchett, A. R. Jude, L. L. Providence, O. S. Andersen, and D. V. Greathouse. 2000. Neighboring aliphatic/aromatic side chain interactions between residues 9 and 10 in gramicidin channels. *Biochemistry.* 39:2235–2242.

Koeppe II, R. E., J. A. Killian, and D. V. Greathouse. 1994. Orientations of the tryptophan 9 and 11 side chains of the gramicidin channel based on deuterium nuclear magnetic resonance spectroscopy. *Biophys. J.* 66:14–24.

Koeppe, R. E., J. A. Killian, T. C. Vogt, B. de Kruijff, M. J. Taylor, G. L. Mattice, and D. V. Greathouse. 1995. Palmitoylation-induced conformational changes of specific side chains in the gramicidin transmembrane channel. *Biochemistry.* 34:9299–9306.

Ladokhin, A. S., and S. H. White. 2001. αs and τs of tryptophan fluorescence in membranes. *Biophys. J.* 81:1825–1827.

Lau, E. Y., and J. T. Gerig. 1997. Effects of fluorine substitution on the structure and dynamics of complexes of dihydrofolate reductase (*Escherichia coli*). *Biophys. J.* 73:1579–1592.

Lazo, N. D., W. Hu, and T. A. Cross. 1995. Low-temperature solid-state ^{15}N NMR characterization of polypeptide backbone librations. *J. Magnet. Reson. B.* 107:43–50.

Lazo, N. D., W. Hu, K.-C. Lee, and T. A. Cross. 1993. Rapidly-frozen polypeptide samples for characterization of high definition dynamics by solid-state NMR spectroscopy. *Biochem. Biophys. Res. Commun.* 197:904–909.

Lee, K.-C., W. Hu, and T. A. Cross. 1993. ^{2}H NMR determination of the global correlation time of the gramicidin channel in a lipid bilayer. *Biophys. J.* 65:1162–1167.

Lee, K.-C., S. Huo, and T. A. Cross. 1995. Lipid-peptide interface: valine conformation and dynamics in the gramicidin A channel. *Biochemistry.* 34:857–867.

Luck, L. A., and C. Johnson. 2000. Fluorescence and ^{19}F NMR evidence that phenylalanine, 3-L-fluorophenylalanine and 4-L-fluorophenylalanine bind to the L-leucine specific receptor of *Escherichia coli*. *Protein Sci.* 9:2573–2576.

Luck, L. A., J. E. Vance, T. M. O'Connell, and R. E. London. 1996. ^{19}F NMR relaxation studies on 5-fluorotryptophan- and tetradeutero-5-fluorotryptophan-labeled *E. coli* glucose/galactose receptor. *J. Biomol. N.M.R.* 7:261–272.

Macdonald, P. M., and J. Seelig. 1988. Dynamic properties of gramicidin A in phospholipid membranes. *Biochemistry.* 27:2357–2364.

Marassi, F. M., and S. J. Opella. 1998. NMR structural studies of membrane proteins. *Curr. Opin. Struct. Biol.* 8:640–648.

Maruyama, T., and H. Takeuchi. 1998. Raman linear intensity difference of membrane-bound peptides: indole ring orientations of tryptophans 11 and 13 in the gramicidin A transmembrane channel. *Biospectroscopy.* 4:171–184.

McDowell, L., M. Lee, R. A. McKay, K. S. Anderson, and J. Schaefer. 1996. Intersubunit communication in tryptophan synthase by carbon-13 and fluorine-19 REDOR NMR. *Biochemistry.* 35:3328–3334.

McDowell, L. M., S. M. Holl, S. Qian, E. Li, and J. Schaefer. 1993. Intertryptophan distances in rat cellular retinol binding protein II by solid-state NMR. *Biochemistry.* 32:4560–4563.

Mehring, M. 1983. Principles of High Resolution NMR in Solids. Springer, New York.

Mehring, M., R. G. Griffin, and J. S. Waugh. 1971. [19]F shielding tensors from coherently narrowed NMR powder spectra. *J. Chem. Phys.* 55:746–755.

Morein, S., I. R. Koeppe, G. Lindblom, B. de Kruijff, and J. A. Killian. 2000. The effect of peptide/lipid hydrophobic mismatch on the phase behavior of model membranes mimicking the lipid composition in *Escherichia coli* membranes. *Biophys. J.* 78:2475–2485.

Mousson, F., V. Beswick, Y. M. Coic, F. Baleux, T. Huynh-Dinh, A. Sanson, and J. M. Neumann. 2001. Concerted influence of key amino acids on the lipid binding properties of a single-spanning membrane protein: NMR and mutational analysis. *Biochemistry.* 40:9993–10000.

Murphy 3rd, O. J., F. A. Kovacs, E. L. Sicard, and L. K. Thompson. 2001. Site-directed solid-state NMR measurement of a ligand-induced conformational change in the serine bacterial chemoreceptor. *Biochemistry.* 40:1358–1366.

Nehring, J., and A. Saupe. 1970. Anisotropies of the ^{19}F chemical shifts in fluorobenzene compounds from NMR in liquid crystals. *J. Chem. Phys.* 52:1307–1310.

Nicholson, L. K., T. Asakura, M. Demura, and T. A. Cross. 1993. A method for studying the structure of uniaxially aligned biopolymers using solid-state ^{15}N-NMR: application to *Bombyx mori* silk fibroin fibers. *Biopolymers.* 33:847–861.

Nicholson, L. K., Q. Teng, and T. A. Cross. 1991. Solid-state nuclear magnetic resonance derived model for dynamics in the polypeptide backbone of the gramicidin A channel. *J. Mol. Biol.* 218:621–637.

Oh, D., S. Y. Shin, S. Lee, J. H. Kang, S. D. Kim, P. D. Ryu, K. S. Hahm, and Y. Kim. 2000. Role of the hinge region and the tryptophan residue in the synthetic antimicrobial peptides, cecropin A(1–8)-magainin 2(1–12) and its analogues, on their antibiotic activities and structures. *Biochemistry.* 39:11855–11864.

Okada, A., T. Miura, and H. Takeuchi. 2001. Protonation of histidine and histidine-tryptophan interaction in the activation of the M2 ion channel from influenza a virus. *Biochemistry.* 40:6053–6060.

Opella, S. J. 1997. NMR and membrane proteins. *Nat. Struct. Biol. N.M.R.* Suppl.:845–848.

Pascal, S. M., and T. A. Cross. 1993. High-resolution structure and dynamic implications for a double-helical gramicidin A conformer. *J. Biomol. N.M.R.* 3:495–513.

Phillips, L. R., C. D. Cole, R. J. Hendershot, M. Cotten, T. A. Cross, and D. D. Busath. 1999. Noncontact dipole effects on channel permeation: III. Anomalous proton conductance effects in gramicidin. *Biophys. J.* 77:2492–2501.

Pigault, C., A. Follenius-Wund, and M. Chabbert. 1999. Role of Trp-187 in the annexin V-membrane interaction: a molecular mechanics analysis. *Biochem. Biophys. Res. Commun.* 254:484–489.

Reshetnyak, Y. K., and E. A. Burnstein. 2001. Decomposition of protein tryptophan fluorescence spectra into log-normal components: II. The statistical proof of discreteness of tryptophan classes in proteins. *Biophys. J.* 81:1710–1734.

Reshetnyak, Y. K., Y. Koshevnik, and E. A. Burstein. 2001. Decomposition of protein tryptophan fluorescence spectra into Log-normal components: III. Correlation between fluorescence and microenvironment parameters of individual tryptophan residues. *Biophys. J.* 81:1735–1758.

Rinia, H. A., R. A. Kik, R. A. Demel, M. M. Snel, J. A. Killian, J. P. van Der Eerden, and B. de Kruijff. 2000. Visualization of highly ordered striated domains induced by transmembrane peptides in supported phosphatidylcholine bilayers. *Biochemistry.* 39:5852–5858.

Salgado, J., S. L. Grage, L. H. Kondejewski, R. N. McElhaney, R. S. Hodges, and A. S. Ulrich. 2002. Alignment of the antimicrobial β-sheet peptide gramicidin S in membranes: a solid-state ^{19}F-NMR study in oriented lipid bilayers. *J. Biomol. N.M.R.* 21, 191–208.

Scarlata, S. F. 1988. The effects of viscosity on gramicidin tryptophan rotational motion. *Biophys. J.* 54:1149–1157.

Scarlata, S. F. 1991. Effect of increased chain packing on gramicidin-lipid interactions. *Biochemistry.* 30:9853–9859.

Schiffer, M., C. H. Chang, and F. J. Stevens. 1992. The functions of tryptophan residues in membrane proteins. *Protein Eng.* 5:213–214.

Sharpe, S., K. R. Barber, and C. W. Grant. 2000. Val(659)→Glu mutation within the transmembrane domain of ErbB-2: effects measured by ^{2}H NMR in fluid phospholipid bilayers. *Biochemistry.* 39:6572–6580.

Sharpe, S., and C. W. Grant. 2000. A transmembrane peptide from the human EGF receptor: behaviour of the cytoplasmic juxtamembrane domain in lipid bilayers. *Biochim. Biophys. Acta.* 1468:262–272.

Snyder, L. C. 1965. Analysis of nuclear magnetic resonance spectra of molecules in liquid-crystal solvents. *J. Chem. Phys.* 43:4041–4050.

Spohn, K. H., R. Kimmich, S. Sharpe, and C. W. Grant. 1983. Characterization of the mobility of various chemical groups in the purple membrane of *Halobacterium halobium* by ^{13}C, ^{31}P, and ^{2}H solid state NMR. *Biochem. Biophys. Res. Commun.* 114:713–720.

Sun, Z.-Y., E. A. Pratt, and C. Ho. 1996. ^{19}F-labeled amino acids as structural and dynamic probes in membrane-associated proteins. Biomedical Frontiers of Fluorine Chemistry. I. Ojima, J. R. M., J. T. Welch, editors. Biomedical Frontiers of Fluorine Chemistry, ACS Symposium Series, American Chemical Society. 296–310.

Takeuchi, H., Y. Nemoto, and I. Harada. 1990. Environments and conformations of tryptophan side chains of gramicidin A in phospholipid bilayers studied by Raman spectroscopy. *Biochemistry.* 29:1572–1579.

Thompson, N., G. Thompson, C. Cole, M. Cotten, T. A. Cross, and D. Busath. 2001. Noncontact dipole effects on channel permeation: IV. Kinetic model of 5F-Trp13 gramicidin A currents. *Biophys. J.* 81: 1245–1254.

Townsley, L. E., W. A. Tucker, S. Sham, and J. F. Hinton. 2001. Structures of gramicidins A, B, and C incorporated into sodium dodecyl sulfate micelles. *Biochemistry.* 40: 11676–11686.

Ulrich, A. S. 2000. High resolution solid state NMR, ^{1}H, ^{19}F. *In* Encyclopedia of Spectroscopy and Spectrometry. J. Lindon, G. Tranter, and J. Holmes, editors. Academic Press, London. 813–825.

Ulrich, A. S., and S. L. Grage. 1998. ^{2}H NMR. Solid State NMR. I. Ando and T. Asakura, editors. Elsevier Science, Amsterdam. 190–211.

Ulrich, A. S., M. P. Heyn, and A. Watts. 1992. Structure determination of the cyclohexene ring of retinal in bacteriorhodopsin by solid-state deuterium NMR. *Biochemistry.* 31:10390–10399.

Ulrich, A. S., I. Wallat, M. P. Heyn, and A. Watts. 1995. Re-alignment of the retinal chromophore in the M-photointermediate of bacteriorhodopsin. *Nat. Struct. Biol.* 2:190–192.

Ulrich, A. S., and A. Watts. 1993. ^{2}H-NMR lineshapes of immobilized uniaxially oriented membrane proteins. *Solid State N.M.R.* 2:21–36.

Ulrich, A. S., and A. Watts. 1994. Molecular response of the lipid headgroup to bilayer hydration monitored by ^{2}H-NMR. *Biophys. J.* 66: 1441–1449.

Ulrich, A. S., A. Watts, I. Wallat, and M. P. Heyn. 1994. Distorted structure of the retinal chromophore in bacteriorhodopsin resolved by ^{2}H-NMR. *Biochemistry.* 33:5370–5375.

Wallace, B. A., and R. W. Janes. 1999. Tryptophans in membrane proteins: x-ray crystallographic analyses. *Adv. Exp. Med. Biol.* 467:789–799.

Watts, A., A. S. Ulrich, and D. A. Middleton. 1995. Solid-state NMR studies of membrane proteins. *Mol. Membr. Biol.* 12:233–246.

Yim, C. T., and D. F. R. Gilson. 1968. Analysis of the proton and fluorine magnetic resonance spectra of 1,3,5-trifluorobenzene dissolved in a nematic liquid crystal. *Can. J. Chem.* 46:2783–2786.

Zemsky, J., E. Rusinova, Y. Nemerson, L. A. Luck, and J. B. Ross. 1999. Probing local environments of tryptophan residues in proteins: comparison of ^{19}F nuclear magnetic resonance results with the intrinsic fluorescence of soluble human tissue factor. *Proteins.* 37:709–716.